

# Synthesis and magnetic properties of $\text{LaFe}_{13-x-y}\text{M}_x\text{Si}_y\text{N}_3$ nitrides

A. Thayer,<sup>a</sup> I. Hlova,<sup>b</sup> Y. Mudryk,<sup>b\*</sup> X. Liu,<sup>b</sup> V.K. Pecharsky<sup>a,b</sup>

<sup>a</sup> Department of Materials Science and Engineering, Iowa State University, Ames, IA 50011

<sup>b</sup> Ames Laboratory of US DOE, Iowa State University, Ames, IA 50011

\*Corresponding Authors: slavkomk@ameslab.gov

## Abstract

Single-phase  $\text{LaFe}_{13-x-y}\text{M}_x\text{Si}_y\text{N}_3$  compounds ( $\text{M} = \text{Mn}$ ) were synthesized by subjecting intermetallic precursors to the ammonia flow at 623 K for 4 hours. The nitrides derived from Si-poor ( $y \leq 3$ ) cubic intermetallics retain the  $\text{NaZn}_{13}$ -type crystal structure and show considerable ( $\sim 3\%$ ) lattice expansion compared to the nitrogen-free materials. The temperatures of the magnetic ordering transitions, all of which are second order, increase by  $\sim 200$  K as a result of nitrogenation, and all nitrides exhibit rather weak and broad magnetocaloric effects. The nitrides are stable below 750 K, but they begin to lose nitrogen above this temperature, fully decomposing above 1050 K. The nitrogenation of the tetragonal  $\text{LaFe}_9\text{Si}_4$  results in the decomposition of the intermetallic phase and formation of the  $\text{Fe}_3\text{N}$  compound together with unidentified amorphous phase(s).

## Introduction

$\text{LaFe}_{13-x-y}\text{M}_x\text{Si}_y$  compounds, where M is Mn or Co, and their hydrides are among the most promising currently known materials exhibiting the giant magnetocaloric effect [1-10]. The excellent magnetothermal behaviors of the  $\text{LaFe}_{13-y}\text{Si}_y$  parents are known for several decades [1, 2], and it is only natural that some representatives of the extended  $\text{LaFe}_{13-x-y}\text{M}_x\text{Si}_y$  family (henceforth referred jointly as the 1:13 family) were tested as working bodies in a number of proof-of-principle magnetocaloric heat pump prototypes, showing encouraging results [11,12]. The undoped  $\text{LaFe}_{13-y}\text{Si}_y$  materials have a number of desirable characteristics, such as strong magnetocaloric effects, relatively low hysteresis losses, low toxicity, and their synthesis protocols, though somewhat complicated, are well established. At the same time, while their constituent elements are quite abundant and, therefore, less costly when compared, for example, to  $\text{Gd}_5\text{Si}_2\text{Ge}_2$  [13] or  $\text{FeRh}$  [14], the 1:13 parent alloys must be doped with either cobalt or hydrogen to increase their magnetic ordering temperatures ( $T_C$ ) from around 200 K to room temperature. Cobalt is one of the handful of critical elements, supplies of which could be unreliable. Hydrogen, is, of course, abundant, but the need for precise hydrogenation through gas-solid reactions, adds complexity to the already tedious synthesis.

The 1:13 compounds with  $\sim 1.2 < y_{\text{Si}} < \sim 1.8$  are itinerant electron metamagnetic (IEM) systems, where the magnetic ordering temperature may often be controlled by manipulating phase volume. In general, unit-

cell volume expansion increases  $T_C$  and, conversely,  $T_C$ s of 1:13 phases fall upon volume contraction. For example, substituting La with Ce or Pr (Ce and Pr atoms have smaller effective atomic radii than La), significantly reduces the  $T_C$  [15, 16, 17]. Substituting Fe by other 3d metals (Cr, Mn, Co, Ni) also affects the magnetic ordering of these IEM compounds due to element-specific modification of the electronic structure [9, 10, 16, 18, 19]. Among them, Co is the only 3d metal that, when substituted for Fe, increases  $T_C$  of  $\text{LaFe}_{13-x-y}\text{Co}_x\text{Si}_y$  alloys at fixed  $y$  [18, 19]. The transition, however, devolves from first- to second-order as  $x_{\text{Co}}$  increases, halving the magnetocaloric effect (magnetic field-induced entropy changes) compared to those observed when  $x_{\text{Co}} = 0$ . Hydrogenation of  $\text{LaFe}_{13-y}\text{Si}_y$  alloys, on the other hand, preserves the first-order nature of the phase transformation and the giant MCE, while raising  $T_C$  up to 352 K due to lattice expansion [6]. The fully hydrogenated  $\text{LaFe}_{13-y}\text{Si}_y\text{H}_z$  materials contain up to 1.65 hydrogen atoms per formula unit and by varying  $z_{\text{H}}$  one can control the  $T_C$ . Unfortunately, hydrides with less than full hydrogen contents ( $z_{\text{H}} < 1.65$ ) and  $T_C$  at room temperature phase-separate into hydrogen-rich and hydrogen-poor phases with two different  $T_C$ s when held at room temperature for a few days to a few weeks [20]. Thus, 1:13 materials must be fully hydrogenated to ensure their long-term stability. The necessary tuning of  $T_C$ s is achieved by minor substitutions of Fe with Mn, which strongly reduces  $T_C$  of the  $\text{LaFe}_{13-y}\text{Si}_y$  parent [16]. The Si content is adjusted as well, so the actual materials can be described by the chemical formula  $\text{LaFe}_x\text{Mn}_y\text{Si}_z\text{H}_{1.65}$ , where  $11.22 \leq x \leq 11.76$ ,  $0.06 \leq y \leq 0.46$ , and  $1.18 \leq z \leq 1.32$ , making these complex intermetallic hydrides useful over the 270 – 340 K temperature range [21].

Similar to hydrogen, interstitial nitrogen also increases the Curie temperatures of 1:13 alloys [22, 23]. We are aware of a few attempts to develop hard-magnetic properties in both  $\text{LaFe}_{13-y}\text{Si}_y$  [22, 23] and  $\text{LaFe}_{13-y}\text{Al}_y$  compounds [24, 25] by nitrogenating them with gaseous nitrogen. The aluminum-containing compound was fully nitrogenated, forming  $\text{LaFe}_{10.8}\text{Al}_{2.2}\text{N}_3$  [24]. Nitrogenation of  $\text{LaFe}_{13-y}\text{Si}_y$  with  $\text{N}_2$  proved to be more challenging: several studies reported increased lattice parameters and higher magnetic ordering temperatures in  $\text{LaFe}_{13-y}\text{Si}_y\text{N}_z$  compounds, but full nitrogenation, which should reach three nitrogen atoms per formula unit, has never been reported [22, 23]. Correspondingly, magnetic properties of fully nitrogenated  $\text{LaFe}_{13-y}\text{Si}_y$  compounds remain unknown. According to earlier density functional calculations  $\text{LaFe}_{13-y}\text{Si}_y\text{N}_3$  is thermodynamically stable [26], indicating that the synthetic challenge of fully nitrogenating 1:13 silicides is related to the kinetics of the nitrogenation reaction rather than its thermodynamics.

Considering the volume effects alone, one may expect interstitial nitrogen doping to be a more effective parameter controlling  $T_C$  when compared to the interstitial hydrogen due to significantly larger lattice expansion since nitrogen atoms are bigger than hydrogen atoms. However, according to [22] the difference in Curie temperature between, for example,  $\text{LaFe}_{11.5}\text{Si}_{1.5}$  and  $\text{LaFe}_{11.5}\text{Si}_{1.5}\text{N}_{1.6}$  alloys is only 80

K, despite the fact that the lattice parameter  $a$  increases from 11.43 to 11.81 Å ( $\Delta a/a = 3.3\%$ ). Addition of a similar molar amount of hydrogen, on the other hand, doubles the increase in  $T_C$  (from 194 to 352 K,  $\Delta T_C = 162$  K) in the  $\text{LaFe}_{11.5}\text{Si}_{1.5}\text{H}_{1.6}$  hydride, while the increase in the lattice parameter  $a$  is considerably smaller: the maximum change of the lattice parameter  $a$  due to hydrogenation is from 11.468 to 11.601 Å, or  $\Delta a/a = \sim 0.11\%$  [27]. In another study, insertion of 1.3 nitrogen atoms per formula unit of  $\text{LaFe}_{11.7}\text{Si}_{1.3}$  compound increases lattice parameter from 11.467 to 11.733 Å, that is by 2.3%, but  $T_C$  increases from 190 to 233 K [23]. The value of the magnetic field-induced entropy change for the  $\text{LaFe}_{11.7}\text{Si}_{1.3}\text{N}_{1.3}$  compound drops dramatically indicating that first-order phase transition is no longer present in the nitrogenated alloy [23]. A first-principles calculation study indicates that nitrogen insertion changes the nature of the electronic density of states near the Fermi level to the point where first-order IEM behavior is no longer supported [26].

While the literature describing 1:13 nitrides indicates that they are not promising for the emergence of large magnetocaloric effects, there is a number of science questions that remain unanswered. The nitrogen contents in all reported studies were determined gravimetrically by comparing masses before and after the nitrogenation, and they vary broadly from one sample to another, indicating that the nitrogenations were likely incomplete. Correspondingly, the picture of how nitrogen influences the magnetism and crystal structure of 1:13 alloys is far from clear. Another potential difficulty encountered in earlier studies is that using nitrogen gas is not the optimal method for nitrogenation of such alloys. Generally, high pressures and temperatures are required, and nitrogen insertion slows down considerably with time due to poor diffusivity of nitrogen towards the inner layers of that material. Studies show that using gaseous ammonia,  $\text{NH}_3$ , leads to faster and more efficient nitrogenation due to higher reactivity of nitrogen atoms [28]. On the other hand, exposure of 1:13 alloys to  $\text{NH}_3$  during nitrogenation may also lead to simultaneous hydrogenation, which may be beneficial for the kinetics of the chemical reaction as hydrogen expands the lattice, making it easier for the bigger nitrogen atoms to diffuse in, but may also lead to mixed hydride/nitride phase(s), complicating data and their analysis. Therefore, nitrogenation with ammonia must be performed at temperatures where 1:13 hydrides decompose and lose hydrogen but the corresponding nitrides remain stable. Thus, establishing the appropriate synthesis conditions for 1:13 nitrides is a necessary first step towards systematic exploration of their fundamental physical behaviors. With this in mind, we designed a set of experiments to study a) the optimal pathway to synthesize  $\text{LaFe}_{13-y}\text{Si}_y$  nitrides with ammonia; b) examine phase content and structural characteristics of  $\text{LaFe}_{13-y}\text{Si}_y\text{N}_z$ ; and c) probe their magnetic properties and magnetocaloric effects.

## Experimental Methods

Polycrystalline  $\text{LaFe}_{13-y}\text{Si}_y$  precursors with  $y = 1.3, 1.5, 2, 3,$  and  $4,$  as well as  $\text{LaFe}_{11.2}\text{Mn}_{0.3}\text{Si}_{1.5},$  were synthesized using high purity La (99.98 wt.% pure with respect to all other elements in the periodic table) and Fe (99.95 wt.% pure), both obtained from the Materials Preparation Center of the Ames Laboratory. Si (99.9995 wt.% pure) and Mn (99.95 wt.% pure) were purchased from Alfa Aesar. All components were weighed out in desired stoichiometric proportions except Mn, which was taken with a 3 wt.% excess due to its volatility, and then arc-melted on a water-cooled copper hearth in a high-purity argon atmosphere backfilled to between 5–10 in Hg. The buttons weighing 3 g each were flipped and re-melted four times to ensure homogeneity. Weight losses after the arc-melting were less than 0.5%. Afterwards, the samples were wrapped in a Ta foil, sealed in helium-filled quartz ampules, and heat treated at 1100–1150 °C for 2–4 days. For nitrogenation, the as-annealed materials were ground in an agate mortar, screened to select particle size  $<32 \mu\text{m},$  placed in quartz boats, and loaded into a gas-flow reactor inside a tube furnace; then the reactor was evacuated. Nitrogenation was performed with ammonia ( $\text{NH}_3$ ) flow of  $250 \text{ cm}^3/\text{min}$  at temperatures ranging between 300–450 °C for various time periods.

After nitrogenation, recovered powders were stored in an argon filled glove box as a precaution, although no evidence of reaction with atmosphere was observed. Powder X-ray diffraction (XRD) measurements were performed on a PANalytical X'Pert Pro powder diffractometer using  $\text{Cu K}\alpha_1$  radiation with a  $0.02^\circ$   $2\theta$  step between 10 and 80 degrees of  $2\theta.$  The powder XRD patterns obtained before and after the nitrogenation were analyzed using full-profile Rietveld refinement (Rietica LHPM, [29]). Magnetic measurements were performed in a Quantum Design Physical Property Measurement System (PPMS) equipped with a Vibrating Sample Magnetometer (VSM) option. Measurements were performed in applied magnetic fields up to 50 kOe between 5 and 300 K (before nitrogenation) and above 300 K for fully nitrogenated samples. The isofield  $M(T)$  data were measured as functions of temperature at selected constant magnetic fields; the magnetocaloric properties were determined from the  $M(T)$  data using protocol described in detail in Ref. [30]. The nitrides were also analyzed using magnetic thermogravimetry (mTGA) at a heating rate of 20 K/min, between 35 and 900 °C during heating, followed by cooling down to 155 °C; mTGA was implemented by combining a standard thermogravimetric analyzer (Netzsch STA 449 F3 Jupiter system) and a fixed magnetic field gradient created by an external pair of permanent magnets [31,32]. This makes it possible to qualitatively detect changes in bulk magnetization that occur during magnetic (dis)ordering transitions, where the measured weight varies rapidly due to sharp reduction or increase of the magnetic force, in addition to conventional gravitational force that varies as specimen mass changes. The Netzsch STA 449 F3 Jupiter system performs the differential scanning calorimetry (DSC)

analysis of the same sample concurrently with the mTGA measurement. In addition, a standard TGA scan was performed to calculate nitrogen content from the weight loss during sample decomposition.

## Results

### Synthesis and structural characterization

The powder XRD patterns of the precursor materials synthesized by arc-melting and subsequent annealing (Fig. 1a) indicate phase-pure and nearly phase-pure (when  $y_{\text{Si}} = 1.3$  and  $y_{\text{Si}} = 2$ ) samples with small amounts of  $\alpha$ -Fe impurity noticeable in the latter two cases. The crystal structure of the intermetallic 1:13 compounds changes from the cubic NaZn<sub>13</sub>-type when  $y_{\text{Si}} \leq 3$  to the tetragonal Ce<sub>2</sub>Ni<sub>17</sub>Si<sub>9</sub>-type structure when  $y_{\text{Si}} = 4$ , confirming earlier report [33].

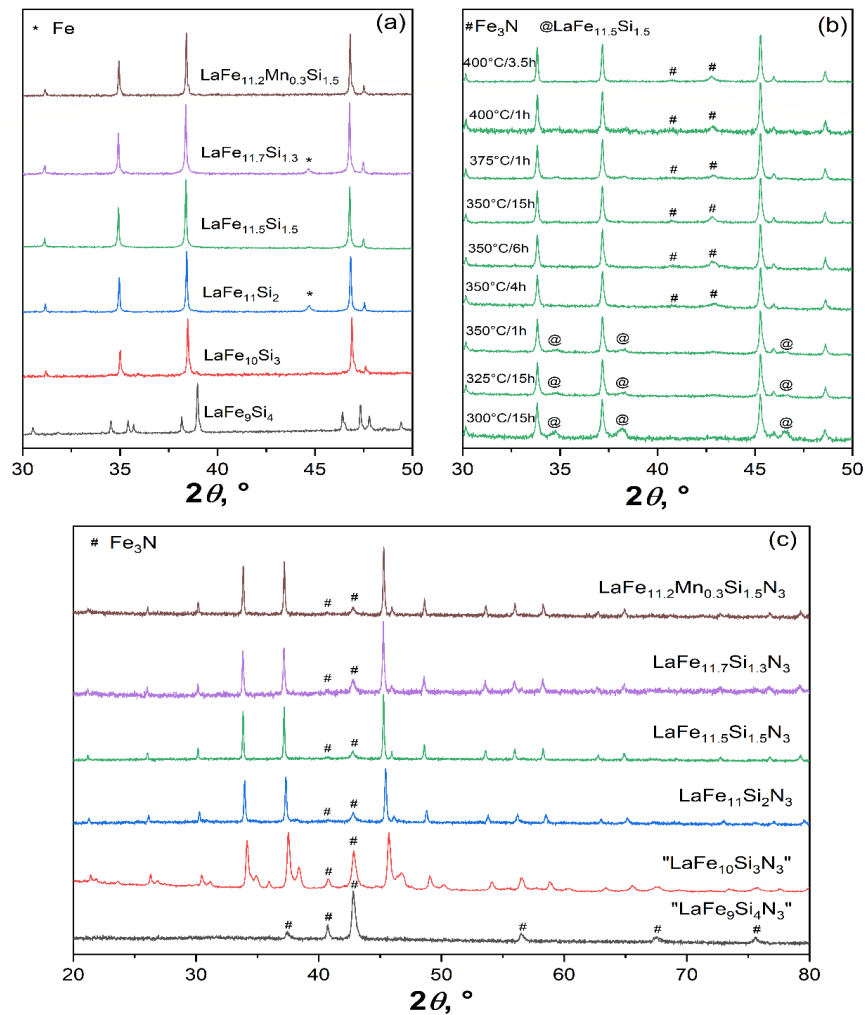


Figure 1. (a) Powder XRD patterns of the 1:13 precursor materials synthesized by arc-melting and homogenization annealing at 1100–1150 °C for 2–4 days. (b) Powder XRD patterns of  $\text{LaFe}_{11.5}\text{Si}_{1.5}$

nitrogenated by flowing ammonia at temperatures and times as marked. (c) Powder XRD patterns after nitrogenation with flowing ammonia for 3.5 h at 400 °C.

Prior to nitrogenation of all materials, the single phase  $\text{LaFe}_{11.5}\text{Si}_{1.5}$  was selected to systematically investigate its nitrogenation with ammonia between 300 and 450 °C to find the optimum synthesis protocol. The powder XRD data of samples nitrogenated at different temperatures (Fig. 1b) indicate that below 350 °C the nitrogenation remains incomplete as evidenced by the presence of characteristic but broad Bragg peaks of the  $\text{LaFe}_{11.5}\text{Si}_{1.5}$  parent, which likely contain unidentified amount of hydrogen. When temperature exceeds 400 °C, the starting material is completely converted to the nitride, however, the emergence of  $\text{Fe}_3\text{N}$  in large concentration (not shown in Fig. 1b) indicates disproportionation of the nitride. The optimal nitrogenation condition, which yields a crystalline nitride with the narrowest Bragg peaks, albeit with a small amount of the  $\text{Fe}_3\text{N}$  impurity present, is flowing gaseous  $\text{NH}_3$  for 3.5 hours while holding the powder at 400 °C. All other precursors have been nitrogenated following this nitrogenation protocol; the powder XRD results are illustrated in Fig. 1c. Powders with the highest concentrations of Si ( $y_{\text{Si}} = 3$  and 4) nitrogenate differently when compared to the rest of the family. When  $y = 3$  the nitrogenation remains incomplete and the amount of  $\text{Fe}_3\text{N}$  is much higher when compared to  $y \leq 2$  materials. For  $\text{LaFe}_9\text{Si}_4$  the only crystalline phase is  $\text{Fe}_3\text{N}$ , indicating practically complete disproportionation, with La and Si likely contained in X-ray amorphous phase(s).

The powder XRD patterns obtained before and after the nitrogenation were analyzed using full-profile Rietveld refinement (Rietica LHPM, [29]) and the results for the nitrogenated samples are shown in Figure 2.  $\text{LaFe}_9\text{Si}_4$  (Figure 2f) is clearly different from the rest of the samples: before nitrogenation it exists as phase-pure  $\text{Ce}_2\text{Ni}_{17}\text{Si}_9$ -type, while the nitrogenated sample reveals the diffraction pattern of phase-pure  $\text{Fe}_3\text{N}$ . In the samples with  $y_{\text{Si}} \leq 2$ , including the Mn-doped material, the main phase retains the  $\text{NaZn}_{13}$ -type cubic structure, and minor second phases are either Fe (for the precursors) or  $\text{Fe}_3\text{N}$  (for the nitrides), Fig. 2a, b, c, e. While the amount of Fe impurities in the precursors is low (<10%), if any (Fig. 1a), Rietveld refinement indicates a significant amount of  $\text{Fe}_3\text{N}$  in the final products, between 15 and 25 wt. %. Despite high backgrounds due to strong fluorescence of Fe, the majority of the refinements converge to low residuals, that is,  $R_p < 2$ ,  $R_{\text{wp}} < 3$ , and  $R_{\text{Bragg}} < 2$  %. The powder XRD pattern of the nitrogenated  $\text{LaFe}_{10}\text{Si}_3$  (Figure 2d) shows poor fit because in addition to the Bragg peaks of the three identified phases,  $\text{LaFe}_{10}\text{Si}_3\text{N}_x$  (49 wt.%),  $\text{LaFe}_{10}\text{Si}_3\text{H}_x$  (27 wt.%), and  $\text{Fe}_3\text{N}$  (24 wt.%), there are Bragg peaks of other phase(s) that we were unable to identify. The formation of the  $\text{LaFe}_{10}\text{Si}_3\text{H}_x$  hydride can be derived from the comparison of the lattice parameters between the precursor and the second phase in the nitrogenated sample (Table S2 of the supporting information).

During the refinements, the Fe/Si ratio was fixed to the nominal, placing the corresponding statistical mixtures of Fe and Si atoms on both 8(b) and 96(i) sites. In addition to refining the unit cell parameters and coordinates of atoms on the 96(i) site, nitrogen occupancy on the 24(d) site was refined, showing full (within 3 least squares standard deviations) occupancy, in agreement with the density functional theory predictions of the stable 1:13 trinitrides [26].

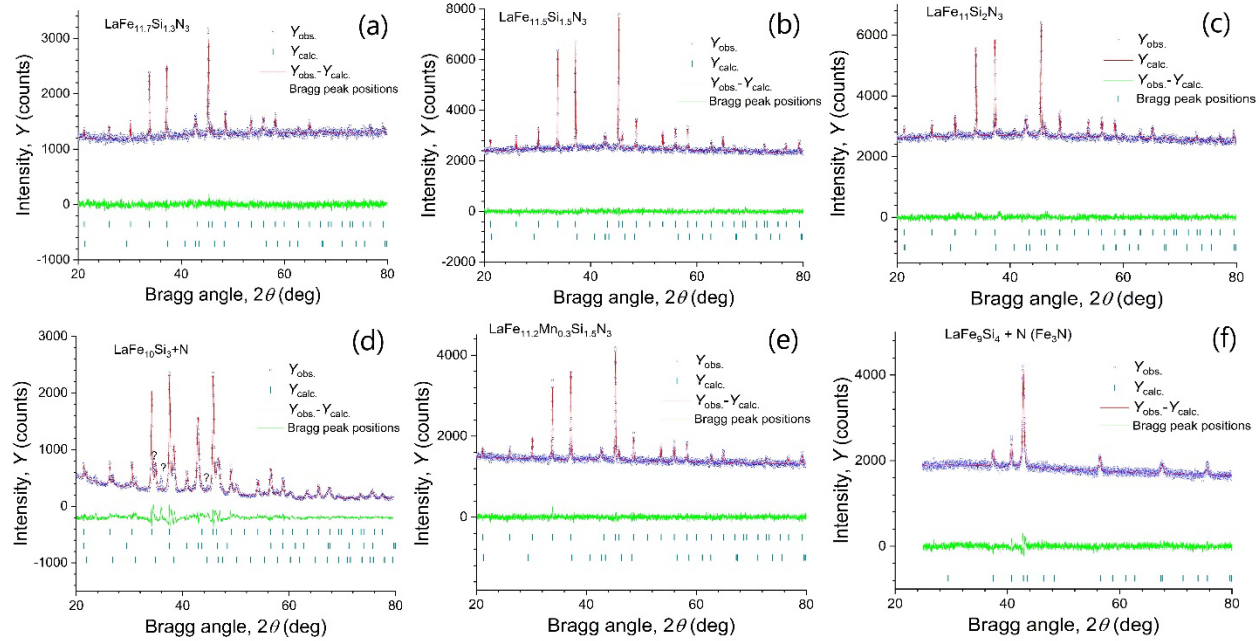


Figure 2. Rietveld-refined powder XRD patterns of the nitrogenated samples with (a)  $y_{\text{Si}} = 1.3$ , (b)  $y_{\text{Si}} = 1.5$ , (c)  $y_{\text{Si}} = 2.0$ , (d)  $y_{\text{Si}} = 3$ , (e)  $y_{\text{Si}} = 1.5$  with minor addition of Mn, and (f)  $y_{\text{Si}} = 4$ . In (a) – (e) the vertical bars at the bottom of the plots indicate positions of the Bragg peaks for  $\text{LaFe}_{13-y}\text{Si}_y\text{N}_3$  (the uppermost sets of bars), followed by the same for  $\text{Fe}_3\text{N}$  and, in panel (d), for  $\text{LaFe}_{10}\text{Si}_3\text{H}_x$ . The vertical bars in panel (f) are positions of the Bragg peaks of  $\text{Fe}_3\text{N}$ .

Lattice parameters of both the precursors and the nitrides are plotted in Figure 3 as functions of Fe content. The linear dependence of the lattice parameter  $a$  observed in the precursor is clearly retained in the nitrides, even though the nitride lattices are expanded due to the insertion of nitrogen atoms, in agreement with literature [22,23]. The Mn doping has little effect on the lattice parameter although, as discussed later, it has a strong impact on the magnetic properties. It is worth noting that in the case of  $\text{LaFe}_{10}\text{Si}_3$  the lattice parameter of the nitride phase is consistent with the linear trend despite the fact the sample is not fully nitrogenated. This suggests that nitrogenation with ammonia consistently yields 1:13 trinitrides, even if a fraction of the material remains not nitrogenated. Further, unlike nitrogenation with nitrogen gas, ammonia appears to be unsuitable for partial nitrogenation, that is, it does not lead to formation of substoichiometric

LaFe<sub>13-y</sub>Si<sub>y</sub>N<sub>3-z</sub> nitrides. The refined lattice parameters of all materials before and after nitrogenation are found in Tables S1 and S2 in the supporting information.

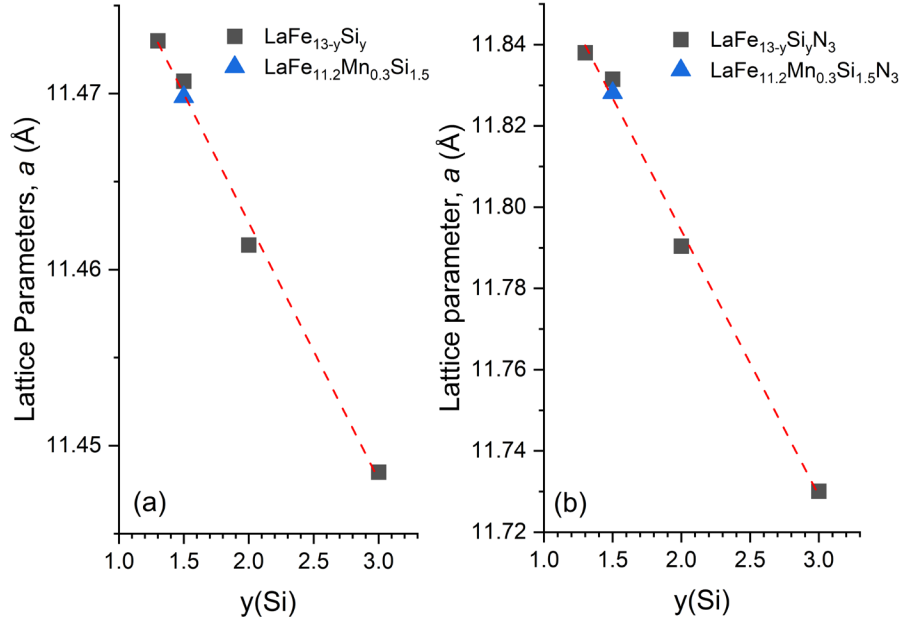


Figure 3. Lattice parameter  $a$  of the NaZn<sub>13</sub>-type cubic phase (a) before and (b) after nitrogenation.

### mTGA and DSC study of LaFe<sub>11.5</sub>Si<sub>1.5</sub>N<sub>3</sub>

The results of mTGA and DSC measurements of the fully nitrogenated LaFe<sub>11.5</sub>Si<sub>1.5</sub> are shown in Figure 4. During heating a sharp drop centered at  $T_C = 405$  K (taken as the minimum of  $\partial\Delta m(T)/\partial T$ , where  $\Delta m(T)$  is the change of effective sample mass recorded as a function of temperature) reflects a sharp change of the magnetic force due to ferromagnetic  $\rightarrow$  paramagnetic transition in LaFe<sub>11.5</sub>Si<sub>1.5</sub>N<sub>3</sub>. A negative change in the slope of  $\Delta m(T)$  that starts around 700 K indicates that a gradual loss of nitrogen begins at this temperature. Upon further heating the effective mass of the sample begins to increase rather quickly around 740 K, which we attribute to the start of disproportionation of LaFe<sub>11.5</sub>Si<sub>1.5</sub>N<sub>3</sub> and formation of a new ferromagnetically ordered phase in agreement with the high-temperature magnetization measurements of the closely related LaFe<sub>11.2</sub>Mn<sub>0.3</sub>Si<sub>1.5</sub>N<sub>3</sub> described later (Figure 6a). The relatively fast increase of  $\Delta m$  becomes a gradual reduction near 900 K, which is followed by another sharp drop observed at  $\sim 1020$  K, signaling that this new, ferromagnetically ordered phase becomes paramagnetic, just below the Curie temperature of the elemental iron,  $T_C = 1043$  K. On cooling, only the magnetic ordering of the Fe-based phase is observed; judging from the Curie temperature, this

ferromagnetic phase has composition close to  $\text{Fe}_9\text{Si}_4$  [34], formation of which is nearly complete around 900 K. Considering the exothermic peak observed in the DSC trace at 1085 K (Figure 4b), this temperature indicates the polymorphic transformation between fcc and bcc lanthanum that contains a few atomic percent of Si [35], thus confirming disproportionation of  $\text{LaFe}_{11.5}\text{Si}_{1.5}\text{N}_3$  upon the loss of nitrogen. A powder XRD pattern of  $\text{LaFe}_{11}\text{Si}_2\text{N}_3$  sample (see Figure S1 in the supporting information), measured at room temperature after a quick heating to 1073 K confirms the gradual loss of nitrogen (the lattice parameter is reduced to  $a = 11.646(2) \text{ \AA}$ ) and the formation of  $\alpha\text{-Fe}$  as the dominant phase. The XRD pattern of the powder heated up to 1173 K (not shown) almost exclusively contains Bragg peaks of  $\alpha\text{-Fe}$ .

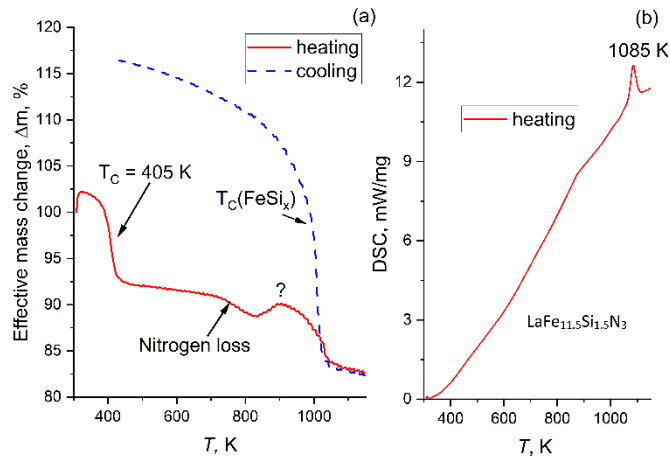


Figure 4. Results of the (a) mTGA and (b) DSC measurements of the  $\text{LaFe}_{11.5}\text{Si}_{1.5}\text{N}_3$  compound.

The mTGA measurements were performed for other nitrogenated samples (excluding the multiphase “ $\text{LaFe}_{10}\text{Si}_3\text{N}_3$ ”) and they are shown in Figure 5. The data for  $\text{LaFe}_9\text{Si}_4$  compound, which does not form a 1:13 nitride (see Figure 1) are shown for comparison. The magnetic disordering transition seen around 400 K on heating is absent in the nitrogenated  $\text{LaFe}_9\text{Si}_4$  sample, confirming that it is a property of the 1:13 nitrides. At the same time, mTGA anomalies that are associated with the high-temperature decomposition and loss of nitrogen are seen in all samples. This indicates that decomposition of 1:13 nitrides is similar to decomposition of  $\text{Fe}_3\text{N}$ . A standard TGA measurement without magnetic field indicates a total  $\sim 5\%$  weight loss during the heating confirming that the nitrides contain three nitrogen atoms per formula unit. We note that mTGA technique is less sensitive compared to conventional magnetometry, and when small amounts of material are used, which is the case for all measured samples except for  $\text{LaFe}_{11.5}\text{Si}_{1.5}\text{N}_3$ , the anomalies are weak and appear smeared. However, it is clear that all 1:13 nitrides without Mn order at approximately same temperature of 405-410 K, while the Mn-containing compound orders at  $\sim 390$  K. This means that  $T_C$  of nitrides is not dependent on the Fe/Si ratio, clearly

contrasting with the behavior of non-nitrogenated precursors, shown below (Figure 6). At the same time, the presence of Mn lowers the  $T_C$  in both the precursor and the nitride. This is an intriguing observation, which points to a disappearance of the IEM and strong sensitivity of  $T_C$  to unit-cell volume in the  $\text{LaFe}_{13-y}\text{Si}_y\text{N}_3$  compounds, while the effect of electronic structure modification due to Fe/Mn substitution is preserved.

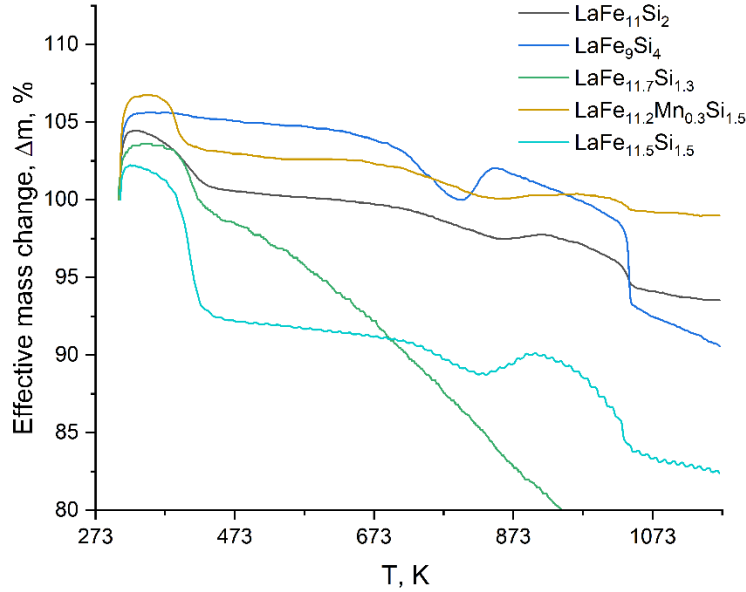


Figure 5. mTGA measurements for  $\text{LaFe}_{13-y}\text{Si}_y\text{N}_3$  nitrides with  $y = 1.3, 1.5, 2, 4,$  and  $\text{LaFe}_{11.2}\text{Mn}_{0.3}\text{Si}_{1.5}\text{N}_3$ .

## Magnetic measurements

### *Before nitrogenation*

The  $M(T)$  behaviors of the precursor specimens were measured prior to nitrogenation between 5 and 300 K in an applied magnetic field of  $B = 0.1$  T to determine their magnetic ordering temperatures,  $T_C$ , defined as the minima of the corresponding  $\partial M(T)/\partial T$ . All samples order ferromagnetically (FM) on cooling; the  $\text{LaFe}_9\text{Si}_4$  compound orders FM at  $T_C = 85$  K; other materials reveal magnetic ordering temperatures ranging from  $T_C = 166$  K for  $\text{LaFe}_{11.2}\text{Mn}_{0.3}\text{Si}_{1.5}$  to  $T_C = 248$  K for  $\text{LaFe}_{10}\text{Si}_3$ . The much lower  $T_C$  of  $\text{LaFe}_9\text{Si}_4$  when compared to other members of the family relates to its different crystal structure. In line with previous reports [1-7], samples with higher Fe content show lower  $T_C$  but more distinctly first-order, hysteretic phase transitions. We note that for  $y_{\text{Si}} = 3$ ,  $T_C$  is lower than expected based on the  $T_C$  vs  $y_{\text{Si}}$  extrapolation. There

is, however, no literature data on  $T_C$  of  $\text{LaFe}_{10}\text{Si}_3$  available for comparison. Figure 6 is a summary of the magnetic ordering transition temperatures of all studied samples with the exception of  $\text{LaFe}_9\text{Si}_4$ , while the underlying  $M(T)$  data are found in the supporting information, Figure S2.

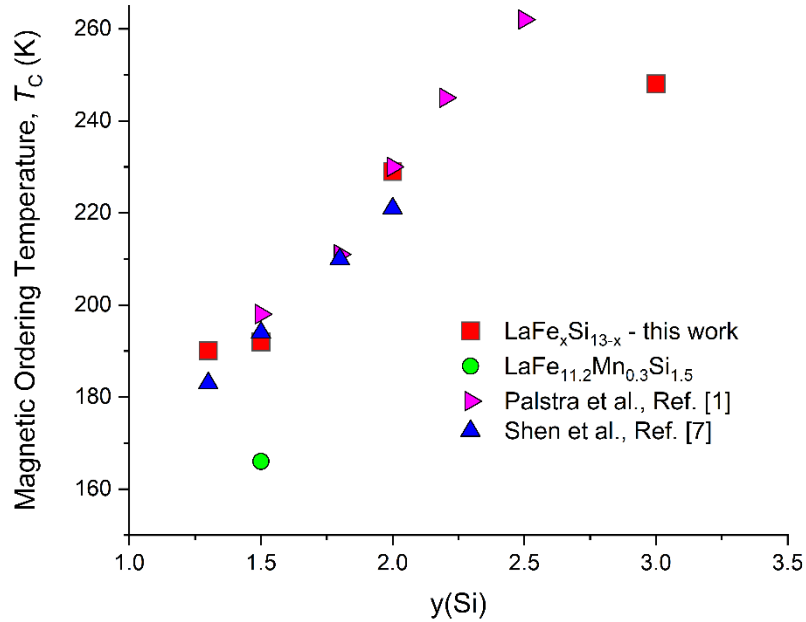


Figure 6. Magnetic ordering temperatures of the prepared 1:13 compounds before nitrogenation.

#### *Nitrogenated $\text{LaFe}_{11.2}\text{Mn}_{0.3}\text{Si}_{1.5}\text{N}_3$*

Several  $\text{La}(\text{Fe},\text{Si})_{13}$  nitrides reported in the past [22,23,24] exhibit broad paramagnetic-ferromagnetic transitions and elevated Curie temperatures, although relationships between  $T_C$  and the content of nitrogen remain unclear, in part because the estimated nitrogen concentrations vary broadly. It is worth noting, however, that in all earlier studies  $T_C$ s of the nitrides were below 400 K. Considering mTGA measurements of  $\text{LaFe}_{13-y}\text{Si}_y\text{N}_3$  illustrated in Fig. 5, the magnetic ordering temperatures of all 1:13 trinitrides are above 400 K. One possible reason is that our samples were nitrogenated using ammonia, resulting in formation of trinitrides –  $\text{La}(\text{Fe},\text{Si})_{13}\text{N}_3$ . The higher content of nitrogen results in larger unit cell volume and higher Curie temperature. At the same time  $T_C$  of the Mn-doped nitride is lower, ~390 K (Fig. 5), and it shows the lowest effective mass loss,  $\Delta m$ , at higher temperatures potentially indicating better thermal stability. Thus, it was chosen to examine magnetic properties and magnetocaloric effect near  $T_C$  using high-temperature VSM measurements.

High-temperature behavior. The Curie temperature of  $\text{LaFe}_{11.2}\text{Mn}_{0.3}\text{Si}_{1.5}\text{N}_3$ , determined as the minimum of  $dM/dT$  measured in  $B = 0.1$  T is 374 K (Figure 7a), reflecting a more than 200 K enhancement from  $T_C =$

166 K recorded before nitrogenation. The  $T_C$  value from the magnetization measurements is lower than 390 K obtained by mTGA method (Figure 5). The difference in  $T_C$  values determined from two different techniques is likely related to the fact that mTGA experiment was performed at a higher heating rate (20 K/min) than in the VSM (2 K/min), further exacerbated by a less efficient heat exchange between the sample and the crucible in the mTGA experiment. Compared with  $T_C = 405$  K of  $\text{LaFe}_{11.5}\text{Si}_{1.5}\text{N}_3$  (Figure 4a), the difference in  $T_C$ s of the corresponding nitrides with  $y_{\text{Si}} = 1.5$  is similar to the same between the two materials before the nitrogenation (166 K for  $\text{LaFe}_{11.2}\text{Mn}_{0.3}\text{Si}_{1.5}$  vs 192 K for  $\text{LaFe}_{11.5}\text{Si}_{1.5}$ ). The ferromagnetic-paramagnetic transition is rather broad and typical of a second-order phase transformation. Heating the nitride above  $\sim 750$  K leads to its partial decomposition seen as a rapid rise of magnetization due to formation of  $\text{FeSi}_x$  [34]. The heating was stopped at 800 K, preventing complete loss of nitrogen, and  $T_C = \sim 320$  K of the remaining nitride on cooling from 800 K becomes much lower than on heating (374 K), reflecting partial loss of nitrogen and formation of a sub-stoichiometric  $\text{LaFe}_{11.2}\text{Mn}_{0.3}\text{Si}_{1.5}\text{N}_{3-\delta}$  nitride. After the cooling measurement was completed, the sample was discarded, and all other measurements described below were performed on a second specimen that was never heated above 500 K to prevent any loss of nitrogen.

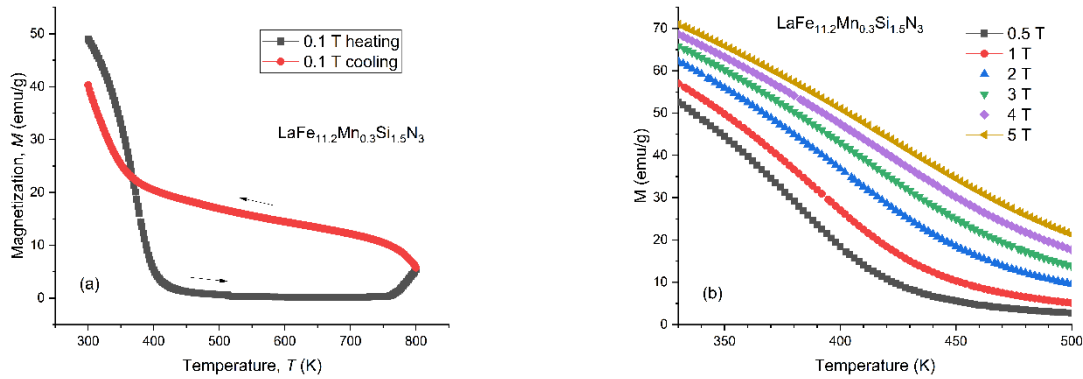


Figure 7. Temperature dependence of dc magnetization of two different  $\text{LaFe}_{11.2}\text{Mn}_{0.3}\text{Si}_{1.5}\text{N}_3$  samples measured (a) in 0.1 T applied magnetic field upon heating and cooling between 300 and 800 K, and (b) in applied magnetic fields of 0.5, 1, 2, 3, 4, and 5 T upon heating between 330 and 500 K.

In higher applied magnetic fields (Fig. 7b), the magnetic ordering transition of the  $\text{LaFe}_{11.2}\text{Mn}_{0.3}\text{Si}_{1.5}\text{N}_3$  compound broadens substantially. This leads to rather low and rapidly declining values of  $|dM/dT|$  and, consequently, low magnetocaloric effect (Fig. 8) calculated using the  $M(T)$  data, some of which are shown in Figure 7b. Even for a magnetic field change of  $\Delta B = 5$  T, the maximum magnetic field-induced entropy change barely reaches  $-2.0$  J/Kg K.

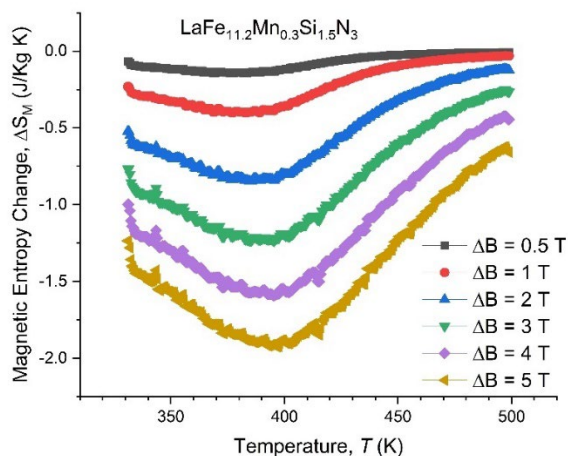


Figure 8. Magnetic field-induced entropy change in the  $\text{LaFe}_{11.2}\text{Mn}_{0.3}\text{Si}_{1.5}\text{N}_3$  compound around  $T_C$  calculated using the  $M(T)$  data, some of which are illustrated in Figure 7b.

The broadness of the transition is indeed the main reason for the low magnetocaloric effect because the magnetization of this compound above room temperature remains substantial (e.g., 72 emu/g or  $1 \mu_B/\text{Fe}$  in  $B = 5 \text{ T}$  at 330 K). Magnetization measured as a function of temperature,  $M(H)$ , reveals soft ferromagnetic behavior (Fig. 9a), in accordance with the cubic symmetry of the nitride. By fitting the high-temperature portion (450-500 K) of the 1 T data to the Curie-Weiss law, we obtained  $\theta_p = 402 \text{ K}$  and effective magnetic moment per transition metal atom  $p_{\text{eff}} = 0.6 \mu_B/(\text{Fe}+\text{Mn})$ , see Figure 9b.

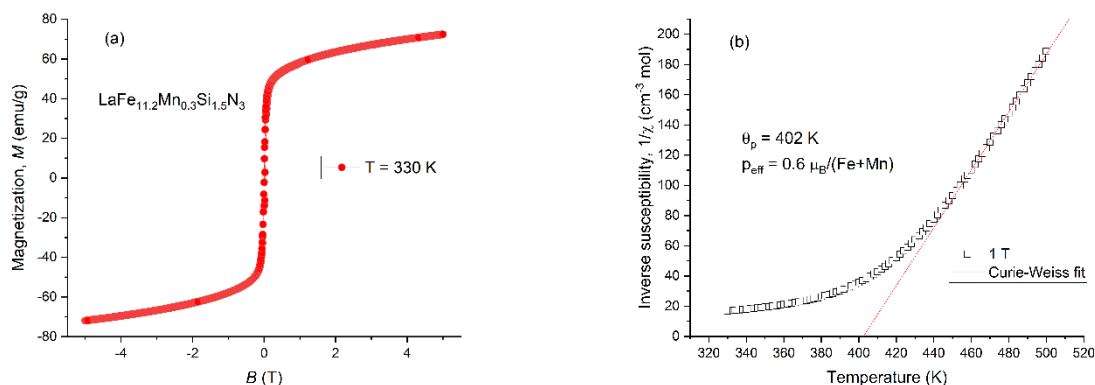


Figure 9. a) Magnetization of  $\text{LaFe}_{11.2}\text{Mn}_{0.3}\text{Si}_{1.5}\text{N}_3$  compound measured at 330 K as a function of applied magnetic field, b) Curie Weiss fit of the 1 T data for the  $\text{LaFe}_{11.2}\text{Mn}_{0.3}\text{Si}_{1.5}\text{N}_3$  sample.

Low-temperature behavior. ac magnetic susceptibility measured between 2 and 250 K (Figure 10) and dc magnetization measured in a 1 kOe applied magnetic field from 2 to 320 K (Figure S3, Supporting Information) do not show any anomalies that may be associated with the ordering of the precursor phase. This confirms that the sample is fully nitrogated, in agreement with the powder XRD data. Furthermore,

dc magnetization data confirm the absence of  $\text{LaFe}_{11.2}\text{Mn}_{0.3}\text{Si}_{1.5}$  hydride, which is expected to order near room temperature for the fully hydrogenated compound or below  $\sim 300$  K when partially hydrogenated. There is a notable divergence between ZFC and FC magnetization developing at low temperatures (Figure S3), and the imaginary component of ac susceptibility shows a peak at 29 K. This phenomenon likely indicates development of hard magnetism or magnetic frustration that may be associated with minor structural distortion and will need to be studied in the future in more detail.

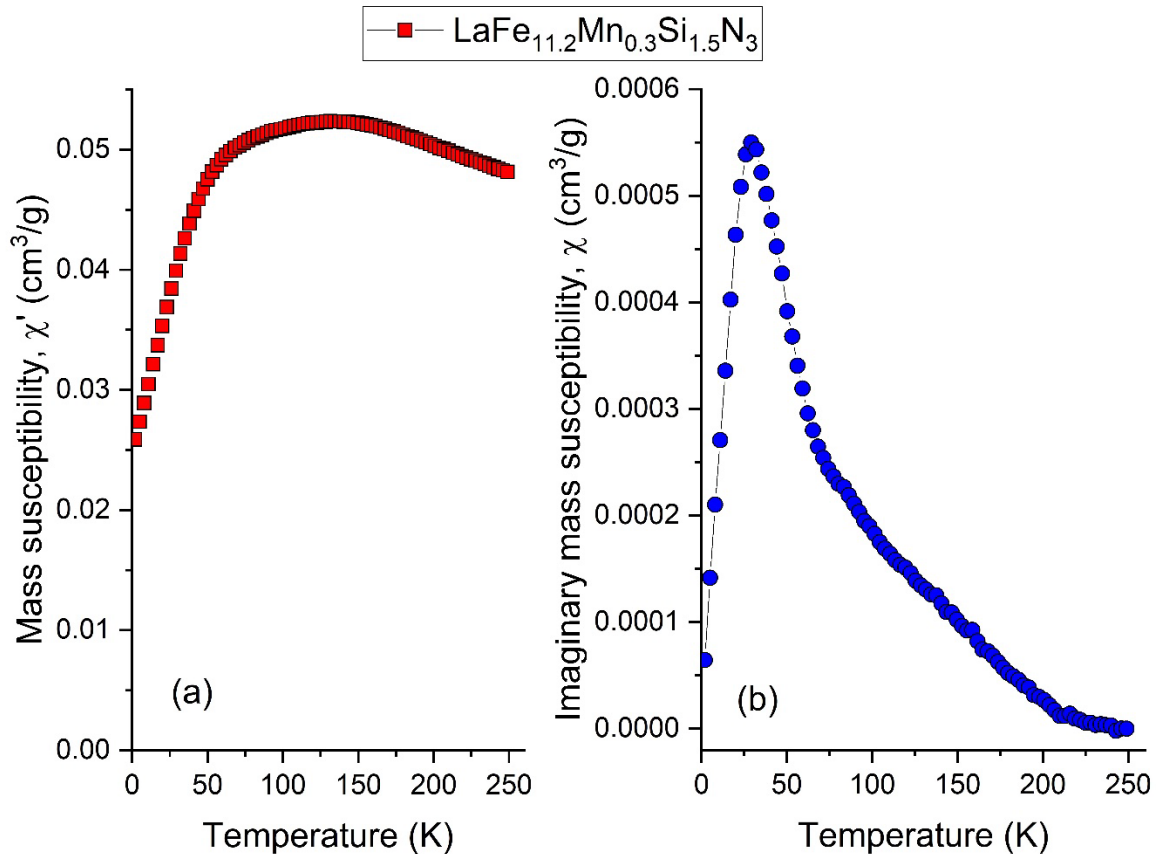


Figure 10. ac magnetic susceptibility of  $\text{LaFe}_{11.2}\text{Mn}_{0.3}\text{Si}_{1.5}\text{N}_3$  measured in  $B_{ac} = 0.0005$  T,  $f = 100$  Hz in the absence of dc bias field on heating after cooling in zero magnetic field: a) real; b) imaginary.

## Conclusions

Thermally-stable up to 750 K nitrides with the general formula  $\text{LaFe}_{13-x-y}\text{M}_x\text{Si}_y\text{N}_3$  and with the cubic  $\text{NaZn}_{13}$ -type structure can be synthesized as nearly single-phase materials through gas-solid reactions with ammonia at 623 K. The nitrogenation of the tetragonal  $\text{LaFe}_9\text{Si}_4$ , on the other hand, leads to a crystalline  $\text{Fe}_3\text{N}$  and unidentified amorphous phase(s). The lattice parameters,  $a$ , of the synthesized trinitrides increase by  $\sim 3\%$  compared to the precursors. The nitrogenation increases ferromagnetic ordering temperatures,  $T_C$ ,

of the nitrogen-free NaZn<sub>13</sub>-type phases by ~200 K, but unlike nitrogen-free intermetallics, T<sub>C</sub>s of the nitrides are independent of the Fe/Si ratio. Partial substitution of Fe with Mn lowers T<sub>C</sub> of the trinitride similarly to the non-nitrogenated precursors. The magnetic ordering transitions in the nitrides are broad, resulting in rather weak magnetocaloric effects peaking at -2.0 J/Kg K for a 0 to 5 T magnetic field change.

## Acknowledgments

Ames Laboratory is operated for the U.S. Department of Energy (DOE) by Iowa State University under Contract No. DE-AC02-07CH11358. This work was supported by the Division of Materials Science and Engineering of the Office of Basic Energy Sciences of the U.S. DOE.

## References

1. T.T.M. Palstra, J.A. Mydosh, G.J. Nieuwenhuys, A.M. van der Kraan, K.H.J. Buschow, Study of the critical behavior of the magnetization and electrical resistivity in cubic La(Fe,Si)<sub>13</sub> compounds, *J. Magn. Magn. Mater.*, **36** (1983) 290.
2. Fujita, Y. Akamatsu, and K. Fukamichi, Itinerant electron metamagnetic transition in La(Fe<sub>x</sub>Si<sub>1-x</sub>)<sub>13</sub> intermetallic compounds, *J. Appl. Phys.*, **85** (1999) 4756.
3. T. Gottschall, K.P. Skokov, M. Fries, A. Taubel, I. Radulov, F. Scheibel, D. Benke, S. Riegg, O. Gutfleisch, Making a cool choice: the materials library of magnetic refrigeration, *Adv. Energy Mater.*, **9** (2019) 1901322.
4. V. Franco, J.S. Blazquez, J.J. Ipus, J.Y. Law, L.M. Moreno-Ramirez, A. Conde, Magnetocaloric effect: from materials research to refrigeration devices, *Prog. Mater. Sci.* **93** (2018) 112.
5. S. Fujieda, A. Fujita, and K. Fukamichi, Large magnetocaloric effect in La(Fe<sub>x</sub>Si<sub>1-x</sub>)<sub>13</sub> itinerant-electron metamagnetic compounds, *Appl. Phys. Lett.*, **81** (2002) 1276.
6. Fujita, S. Fujieda, Y. Hasegawa, and K. Fukamichi, Itinerant-electron metamagnetic transition and large magnetocaloric effects in La(Fe<sub>x</sub>Si<sub>1-x</sub>)<sub>13</sub> compounds and their hydrides, *Phys. Rev. B* **67**, 104416 (2003).
7. B.G. Shen, J.R. Sun, F.X. Hu, H.W. Zhang, and Z.H. Cheng, Recent progress in exploring magnetocaloric materials, *Adv. Mater.*, **21** (2009) 4545.
8. J. Lyubina, R. Schäfer, N. Martin, L. Schultz, and O. Gutfleisch, Novel design of La(Fe,Si)<sub>13</sub> alloys towards high magnetic refrigeration performance, *Adv. Mater.*, **22** (2010) 3735.

9. J. Liu, J.D. Moore, K.P. Skokov, M. Krautz, K. Löwe, A. Barcza, M. Katter, and O. Gutfleisch, Exploring La(Fe,Si)<sub>13</sub>-based magnetic refrigerants towards application, *Scr. Mater.*, **67** (2012) 584.
10. M. Krautz, K. Skokov, T. Gottschall, C.S. Teixeira, A. Waske, J. Liu, L. Schultz, O. Gutfleisch, Systematic investigation of Mn substituted La(Fe,Si)<sub>13</sub> alloys and their hydrides for room-temperature magnetocaloric application, *J. Alloys Compd.*, **598** (2014) 27.
11. S. Jacobs, J. Auringer, A. Boeder, J. Chell, L. Komorowski, J. Leonard, S. Russek, C. Zimm, The performance of a large-scale rotary magnetic refrigerator, *Inter. J. Refrig.*, **37** (2014) 84.
12. J. Tusek, A. Kitanovski, U. Tomc, C. Favero, A. Poredos, Experimental comparison of multi-layered La-Fe-Co-Si and single layered Gd active magnetic regenerators for use in a room-temperature magnetic refrigerator, *Inter. J. Refrig.* **37** (2014) 117.
13. V. K. Pecharsky, K. A. Gschneidner, Jr. *Phys. Rev. Lett.* **78** (1997) 4494.
14. S. A. Nikitin, G. Myalikhulyev, A. M. Tishin, M. P. Annaorazov, K. A. Asatryan, A. L. Tyurin, *Phys. Lett. A* **148** (1990) 363-366.
15. N.-K. Sun, Z.-X. Ren, J. Guo, S.-J. Du, P.-Z. Si, Influence of high-pressure nitrogenation on the structural, magnetic and magnetocaloric properties of La<sub>0.5</sub>Pr<sub>0.5</sub>Fe<sub>11.4</sub>Si<sub>1.6</sub>, *Acta Metall. Sin. (Engl. Lett.)*, **28** (2015) 1382.
16. S. Fujieda, N. Kawamoto, A. Fujita, and K. Fukamichi, Control of working temperature of large isothermal magnetic entropy change in La(Fe<sub>x</sub>TM<sub>y</sub>Si<sub>1-x-y</sub>)<sub>13</sub> (TM = Cr, Mn, Ni) and La<sub>1-z</sub>Ce<sub>z</sub>(Fe<sub>x</sub>Mn<sub>y</sub>Si<sub>1-x-y</sub>)<sub>13</sub>, *Mater. Trans.*, **47** (2006) 482.
17. S. Fujieda, A. Fujita, K. Fukamichi, Enhancement of magnetocaloric effects in La<sub>1-z</sub>Pr<sub>z</sub>(Fe<sub>0.88</sub>Si<sub>0.12</sub>)<sub>13</sub> and their hydrides, *J. Appl. Phys.* **102** (2007) 023907.
18. F.X. Hu, B.G. Shen, J.R. Sun, G.J. Wang, Z.H. Cheng, Very large magnetic entropy change near room temperature in LaFe<sub>11.2</sub>Co<sub>0.7</sub>Si<sub>1.1</sub>, *Appl. Phys. Lett.* **80** (2002) 826.
19. J. D. Moore, K. Morrison, K. G. Sandman, M. Katter, L. F. Cohen, Reducing extrinsic hysteresis in first-order La(Fe,Co,Si)<sub>13</sub> magnetocaloric systems, *Appl. Phys. Lett.* **95** (2009) 252504.
20. C. B. Zimm, S. A. Jacobs, Age splitting of the La(Fe<sub>1-x</sub>Si<sub>x</sub>)<sub>13</sub>H<sub>y</sub> first order magnetocaloric transition and its thermal restoration, *J. Appl. Phys.* **113** (2013) 17A908.
21. V. Basso, M. Küpferling, C. Curcio, C. Bennati, A. Barcza, M. Katter, M. Bratko, E. Lovell, J. Turcaud, L. F. Cohen, *J. Appl. Phys.* **118** (2015) 053907.

22. Z.X. Tang, X.H. Deng, G.C. Hadjipanayis, V. Papaefthymiou, and D.J. Sellmyer, Structural and magnetic properties of LaFe<sub>13-x</sub>Si<sub>x</sub> Nitrides, *IEEE Trans. Magn.* **29** (1993) 2839.
23. M. Bali, M. Rosca, D. Fruchart, D. Gignoux, Effect of interstitial nitrogen on magnetism and entropy change of LaFe<sub>11.7</sub>Si<sub>1.3</sub> compound, *J. Magn. Magn. Mater.* **321** (2009) 123.
24. O. Moze, W. Kockelmann, J.P. Liu, F.R. de Boer, and K.H.J. Buschow, Magnetic structure of LaFe<sub>10.8</sub>Al<sub>2.2</sub> and LaFe<sub>10.8</sub>Al<sub>2.2</sub>N<sub>3</sub> cluster compounds, *J. Appl. Phys.* **87** (2000) 5284.
25. K. Irisawa, A. Fujita, K. Fukamichi, Y. Yamazaki, and Y. Lijima, Influence of nitrogen on the magnetovolume effects in La(Fe<sub>x</sub>Al<sub>1-x</sub>)<sub>13</sub> compounds, *J. Appl. Phys.* **91** (2002) 8882.
26. Z. Gercsi, N. Fuller, K.G. Sandeman, and A. Fujita, Electronic structure, metamagnetism and thermopower of LaSiFe<sub>12</sub> and interstitially doped LaSiFe<sub>12</sub>, *J. Phys. D.: Appl. Phys.*, **51** (2018) 034003.
27. L. Jia et al., Volume dependence of the magnetic coupling in LaFe<sub>13-x</sub>Si<sub>x</sub> based compounds, *Appl. Phys. Lett.* **92** (2008) 101904.
28. M. Katsura, Thermodynamics of nitride and hydride formation by the reaction of metals with flowing NH<sub>3</sub>, *J. Alloys Compd.* **182** (1992) 91-102.
29. B. Hunter, Rietica - A Visual Rietveld Program, International Union of Crystallography Commission on Powder Diffraction Newsletter No. 20, 1998. <http://www.rietica.org>
30. H. Neves Bez, H. Yibole, A. Pathak, Y. Mudryk, V.K. Pecharsky, Best practices in evaluation of the magnetocaloric effect from bulk magnetization measurements, *J. Magn. Magn. Mater.*, **458** (2018) 301.
31. S.D. Norem, M.J. O'Neill, A.P. Gray, The use of magnetic transitions in temperature calibration and performance evaluation of thermogravimetric systems, *Thermochimica Acta*, **1** (1970) 29-38.
32. S.St.J. Warne, P.K. Gallagher, Thermomagnetometry, *Thermochimica Acta*, **110** (1987) 269-279.
33. W. Tang, J. Liang, G. Rao, X. Yan, Study of AC Susceptibility on the LaFe<sub>13-x</sub>Si<sub>x</sub> System, *Phys. Status Solidi A: Appl. Res.*, **141** (1994) 217-222.
34. H. Okamoto, Fe-Si (Iron-Silicon), in *Binary Alloy Phase Diagrams*, 2<sup>nd</sup> Ed., (Ed. T.B. Massalski), **2**, (1990) 1771-1772. <https://matdata.asminternational.org/apd/index.aspx>
35. M.V. Bulanova, P.N. Zheltov, K.A. Meleshevich, P.A. Saltykov, G. Effenberg, J.-C. Tedenac, Lanthanum-silicon system, *J. Alloys Compd.*, **329** (2001) 214-223.